OAK RIDGE NATIONAL LABORATORY LIBRARIES
3 4456 0548412 4

CENTRAL RESEARCH LIBRARY
DOCUMENT COLLECTION

OAK RIDGE NATIONAL LABORATORY

operated by

UNION CARBIDE CORPORATION
NUCLEAR DIVISION
for the
U.S. ATOMIC ENERGY COMMISSION

ORNL-TM-1312
Volume 6

52

STRUCTURAL ANALYSIS OF SHIPPING CASKS

VOL. 6 - IMPACT TESTING OF A LONG CYLINDRICAL LEAD-SHIELDED CASK MODEL

B.B. Klima
L.B. Shappert
W.C.T. Stoddart

OAK RIDGE NATIONAL LABORATORY
CENTRAL RESEARCH LIBRARY
DOCUMENT COLLECTION
LIBRARY LOAN COPY
DO NOT TRANSFER TO ANOTHER PERSON
If you wish someone else to see this document, send in name with document and the library will arrange a loan.

NOTICE This document contains information of a preliminary nature and was prepared primarily for internal use at the Oak Ridge National Laboratory. It is subject to revision or correction and therefore does not represent a final report.

LEGAL NOTICE

This report was prepared as an account of Government sponsored work. Neither the United States, nor the Commission, nor any person acting on behalf of the Commission:

A. Makes any warranty or representation, expressed or implied, with respect to the accuracy, completeness, or usefulness of the information contained in this report, or that the use of any information, apparatus, method, or process disclosed in this report may not infringe privately owned rights; or

B. Assumes any liabilities with respect to the use of, or for damages resulting from the use of any information, apparatus, method, or process disclosed in this report.

As used in the above, "person acting on behalf of the Commission" includes any employee or contractor of the Commission, or employee of such contractor, to the extent that such employee or contractor of the Commission, or employee of such contractor prepares, disseminates, or provides access to, any information pursuant to his employment or contract with the Commission, or his employment with such contractor.

ORNL TM-1312
Vol. 6

Contract No. W-7405-eng-26

CHEMICAL TECHNOLOGY DIVISION

STRUCTURAL ANALYSIS OF SHIPPING CASKS
VOL. 6 – IMPACT TESTING OF A LONG CYLINDRICAL LEAD-SHIELDED CASK MODEL

B. B. Klima, L. B. Shappert, and W. C. T. Stoddart

MARCH 1968

OAK RIDGE NATIONAL LABORATORY
Oak Ridge, Tennessee
operated by
UNION CARBIDE CORPORATION
for the
U.S. ATOMIC ENERGY COMMISSION

OAK RIDGE NATIONAL LABORATORY LIBRARIES
3 4456 0548412 4

CONTENTS

Page

Abstract 1

1. Introduction 1

2. Summary 2

3. The 30-ft Free Drop Test Facility 3

3.1 The Drop Pad 3

3.2 The Tower 3

3.3 The Hoist and Release Mechanism 7

3.4 Data Acquisition 10

4. Cask Tests - ORNL - U. T 10

5. Cask Testing - Franklin Institute 24

6. Analytical Treatment of Lead Movement Under Impact Conditions 24

6.1 End Drop 26

7. Application of Analysis to ORNL-Built 1:7.5 Scale Model of Hallam Cask ... 30

8. Application of Analysis to the Franklin Institute 1:12.5 Scale Model of Hallam Cask 31

9. Acknowledgement 32

STRUCTURAL ANALYSIS OF SHIPPING CASKS VOL. 6 – IMPACT TESTING OF A LONG CYLINDRICAL LEAD-SHIELDED CASK MODEL

B. B. Klima, L. B. Shappert, and W. C. T. Stoddart

ABSTRACT

Settling of lead in lead-filled fissile and radioactive materials shipping casks due to impact was investigated. The cask testing facility at the University of Tennessee is described. Results indicate that when an unbonded cylindrical cask is subjected to an impact, lead will move relative to the steel shell. A mathematical model is developed to quantitatively predict the magnitude of the lead movement. Data acquired in the U.T. Testing Program and during the testing of a smaller model by Franklin Institute confirms the applicability of this developed equation to predict lead movement in an unbonded cask.

1. INTRODUCTION

When it is necessary to ship or transport radioactive material from one place to another, a shielded container or cask must be provided so that the material can be handled without undue exposure of personnel to the radiation. Lead is probably the most frequently used shielding material in this country even though it is low in tensile strength and is easily deformed under accidental impact. It also has a low melting point and in a fire it may melt, resulting in a loss of shielding. A steel inner and outer shell is provided to contain the lead to minimize damage to the lead from impact or fire. These shells are prefabricated and then filled by pouring molten lead into the cavity followed by sealing off the pour holes.

Often, in the past, the heat transfer requirements have been overshadowed by other structural problems. However, second and third generation power reactor fuels will tax heat dissipation abilities of the casks to capacity. A bond between the lead shield and the steel shell may be

desirable to enhance the ability of the cask to dissipate the heat load imposed on it by its contents but it is difficult to pour lead to ensure a metallurgical bond, particularly if the shell is fabricated from stainless steel.

It now appears that the bond may be also desirable to mechanically support the lead as well as to transfer heat. Recent information has been developed which indicates that in a hypothetical accident, movement on impact of lead which is not bonded to its steel shell may create a void resulting in loss of shielding such that allowable dose rates are exceeded.

The present regulations[1] which have been developed to cover shipment of radioactive and fissile material define "hypothetical accident conditions." One of the hypothetical accidents requires the cask to be able to withstand a "free drop" defined below.

Free Drop – A free drop through a distance of 30 ft onto a flat essentially unyielding horizontal surface, striking the surface in a position for which maximum damage is expected.

Facilities to test casks in a 30-ft free drop have been built at the University of Tennessee, Knoxville, Tennessee and are described in this report. Test cask weights are limited to approximately 200 lb.

An analytical procedure has been developed to estimate the extent of the lead movement as a result of a 30-ft free fall if the lead is not bonded to the steel shell. A model was built at ORNL and tested to prove the hypothesis developed. Test work involving a free drop of a smaller model at Franklin Institute Research Laboratories is reviewed.

2. SUMMARY

Data collected as a result of test work with casks confirms the hypothesis that unbonded lead will be displaced as a result of the 30-ft drop specified in the "hypothetical accident." This lead displacement could result in loss of shielding unless adequate provisions are made in the design of the lead cavity.

These data indicate that the length of the contained lead column could be reduced as much as 2.5% as a result of the 30-ft drop.

The data are in good agreement with the values predicted using the equation herein derived for the lead displacement as a result of this "hypothetical accident." Therefore, this equation can be used to properly design the lead cavity so that the loss of shielding can be minimized.

3. THE 30-FT FREE DROP TEST FACILITY

The 30-ft free drop test facility was constructed at the University of Tennessee, Knoxville campus. It is located in the northwest corner of the coal bunker behind the old powerhouse east of Estabrook Hall. This site was chosen because of its isolation from other experimental areas and the general public, as well as because of certain advantageous structural features. The facility is shown in Fig. 1.

3.1 The Drop Pad

In defining the free drop condition, the AEC required that the cask strike a flat, essentially unyielding, horizontal surface. The drop pad, constructed to meet this condition, consists of a reinforced concrete base approximately 7 ft square by 2 ft thick which is surmounted by a centrally located 42 x 34 x 4 in. steel impact surface. The steel plate was imbedded in Portland cement grout in order to be able to insure a level, sound, uniformly-supported surface.

The plan for the reinforced concrete pad is shown in Fig. 2. The drop pad and lower portion of the drop tower are shown in Fig. 3.

3.2 The Tower

A tower of commercially available steel scaffolding was constructed because of its low cost, flexibility of application, and ease of erection.

The scaffolding chosen provides a 35-ft-high tower having a 5-ft-square horizontal section. This tower was anchored to the top of the

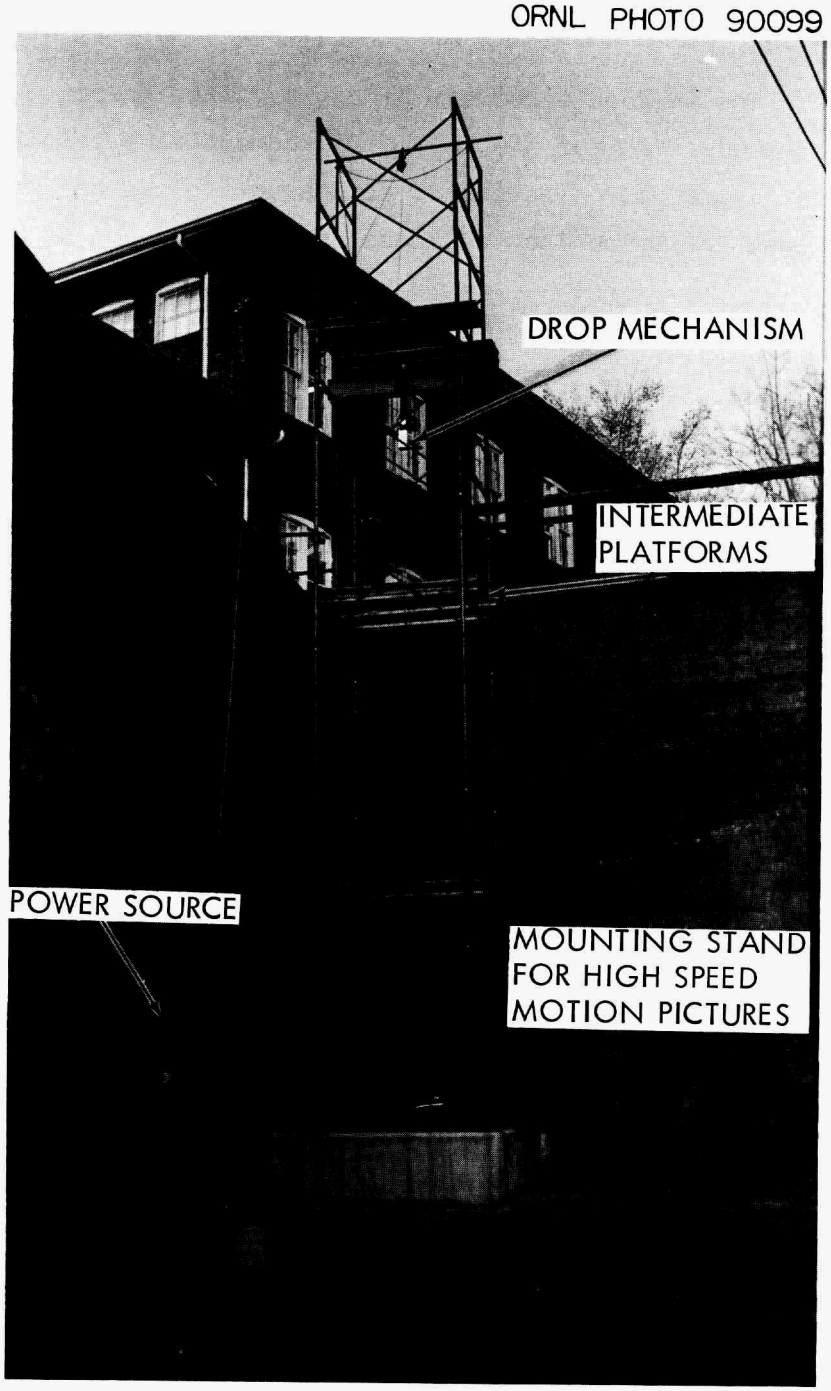

Fig. 1. 30-ft Free Drop Test Facility.

ORNL DWG 67-12871

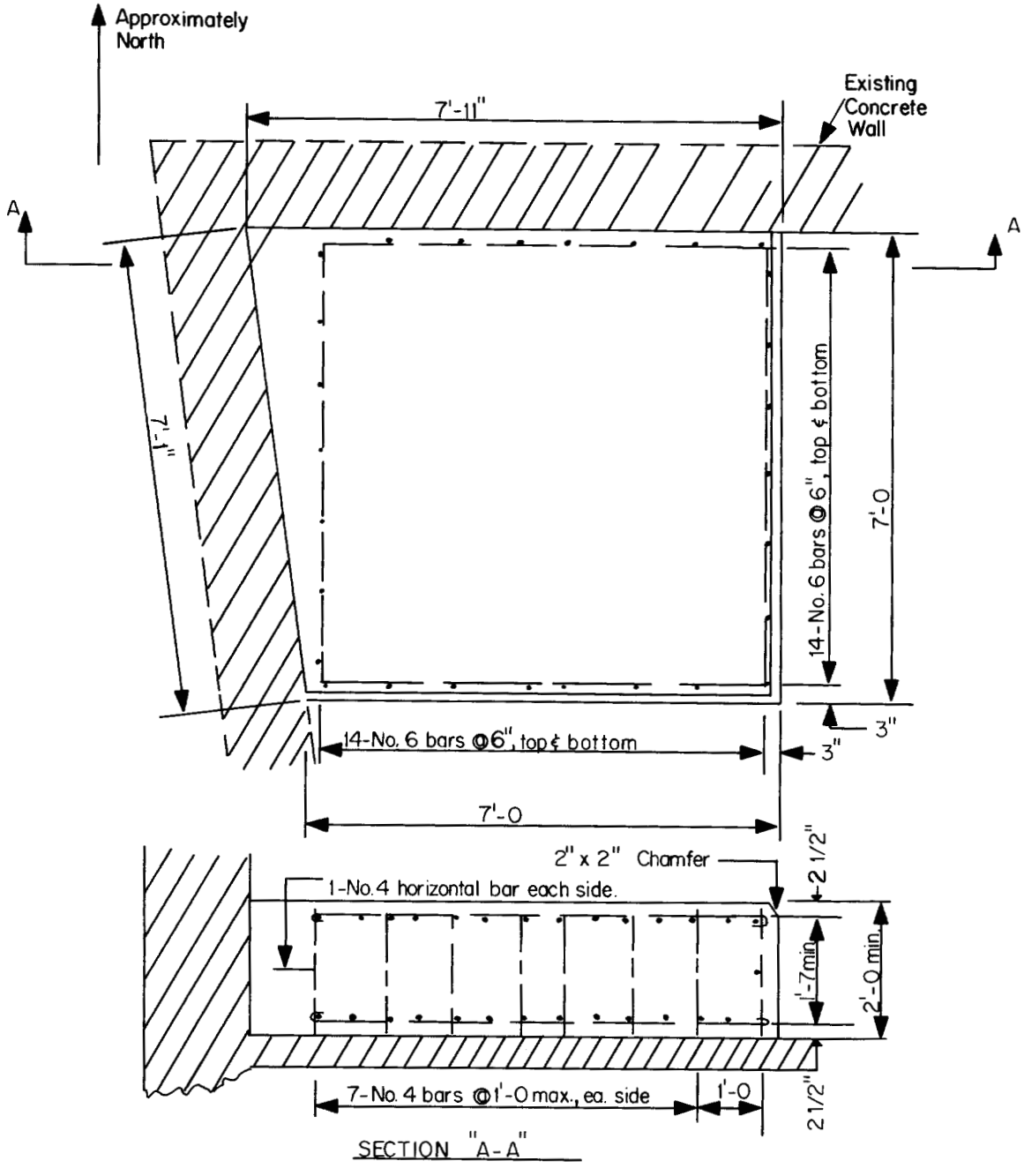

Fig. 2 Reinforced Concrete Pad.

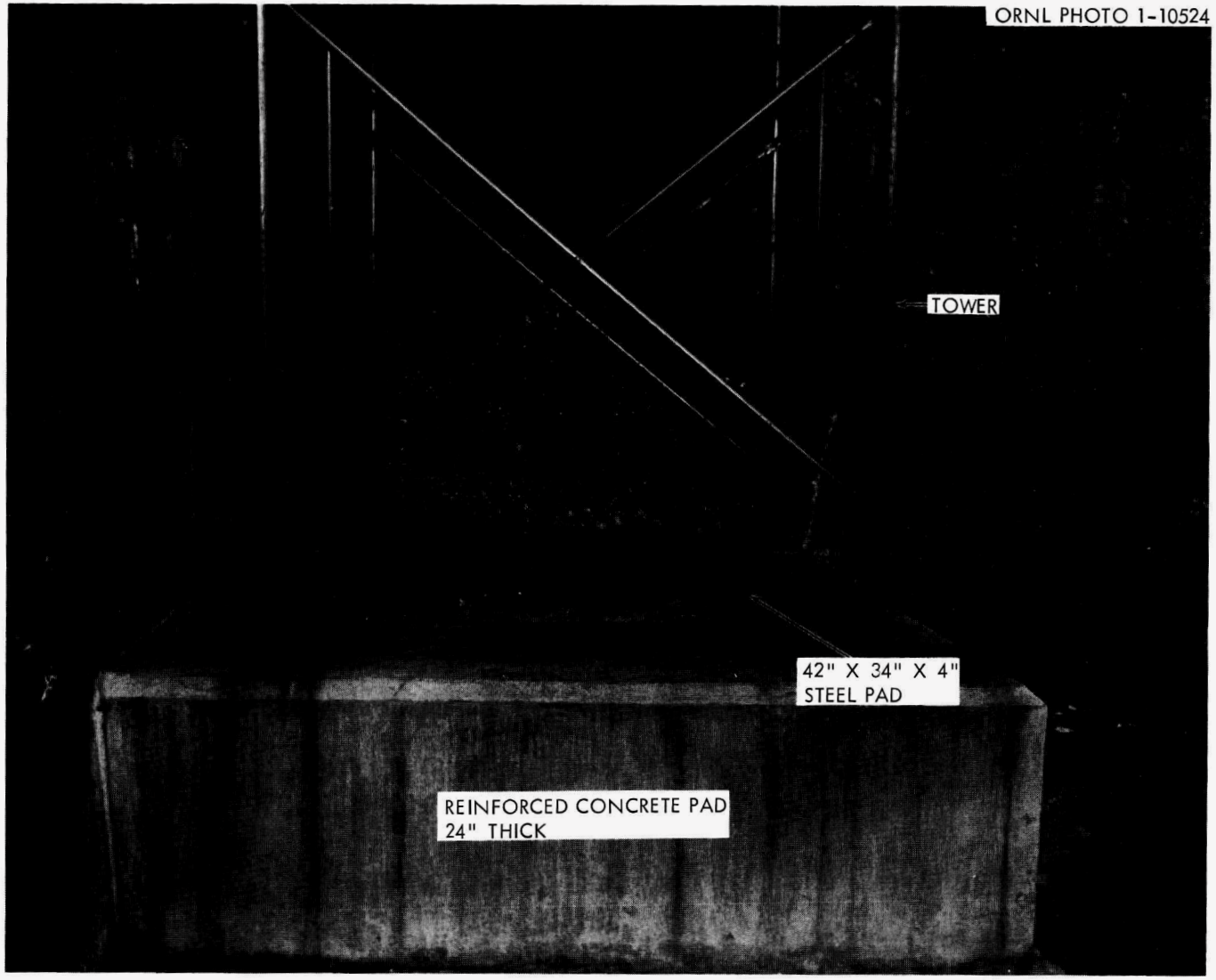

Fig. 3. Drop Pad and Lower Section of the Tower.

existing reinforced concrete walls of the coal bunker, and is equipped with personnel working platforms and a hoisting mechanism. The platforms, installed at heights of approximately 7, 17, and 27 ft above the top of the pad, consist of two center sections hinged to outer sections which are rigidly fixed to the tower. This permits the center sections to be swung out of the path of a test specimen before it is dropped.

3.3 The Hoist and Release Mechanism

The hoist and release mechanism, fabricated from commercially available components, is shown schematically in Fig. 4.

The mechanism is attached to two 2 x 12 in. horizontal wood beams which are attached to the tower. A square carbon steel pipe is bolted to these beams, with its axis in the vertical direction and directly over the center of the steel plate on the impact pad. A winch is bolted to the outside of this pipe at its lower end. Cable is strung from this winch, over a pulley at the top of the pipe, and down through the center of the pipe to the quick release device.

The quick release device (see Fig. 5) is adapted from a commercial quick-release fitting normally used to connect air hoses, and has functioned quite satisfactorily during each test, requiring replacement only when damaged by striking the impact pad during some of the tests. Only the female portion of the quick release device is shown. The male portion is attached to the cable. The quick release device is automatically actuated when it comes in contact with the lower end of the square pipe during the final one inch of travel in hoisting the test specimen into the drop position.

Secondary features of the hoist and release mechanism include a safety device to prevent accidental actuation of the quick release device and an electrical switch (for starting data acquisition equipment) which is automatically closed at the instant of release of the test specimen. Both are operated by an aluminum alloy sleeve which slides on the lower end of the square pipe.

ORNL DWG 67-12866

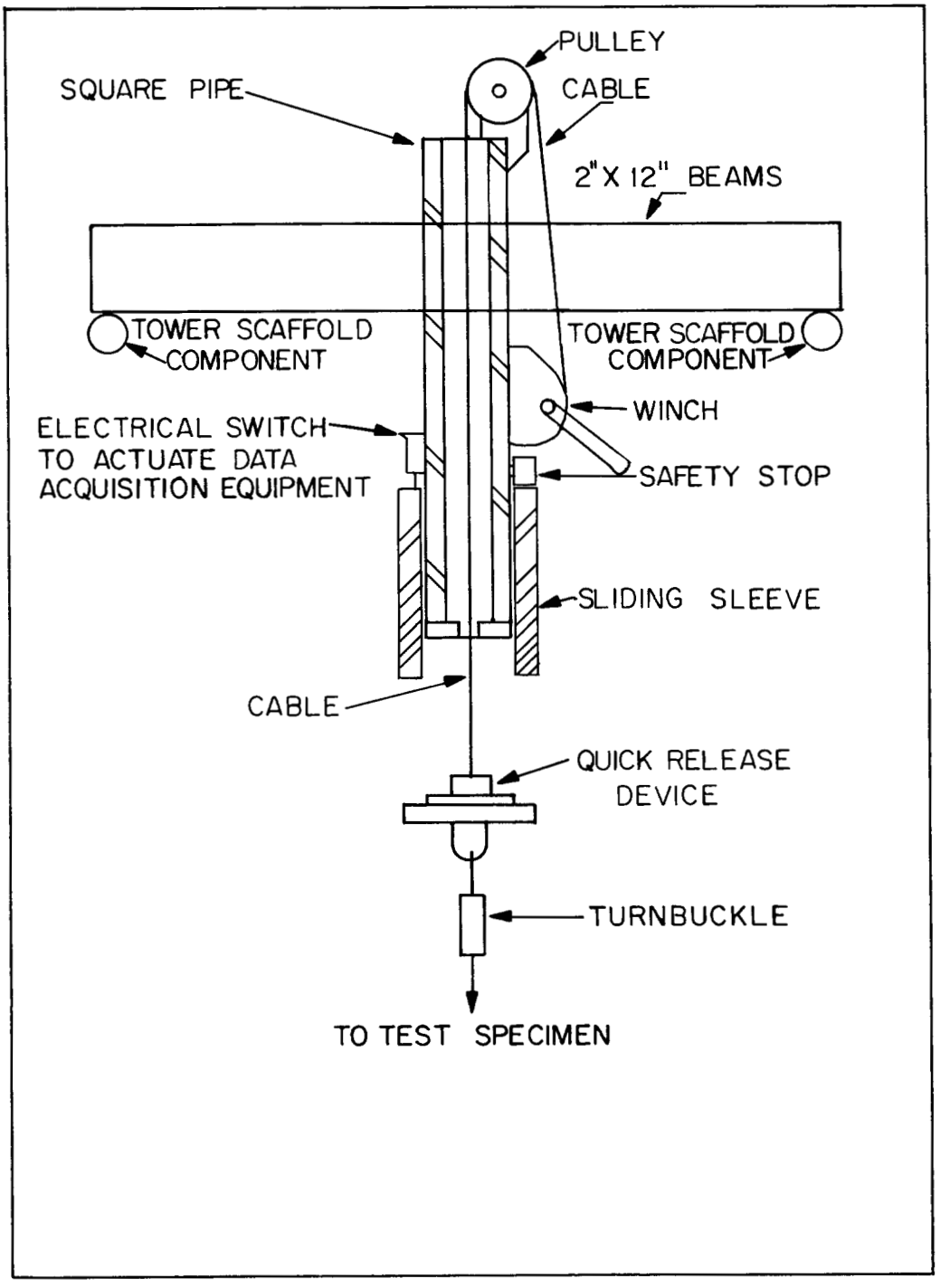

Fig. 4. Schematic Drawing of the Hoist and Release Mechanism.

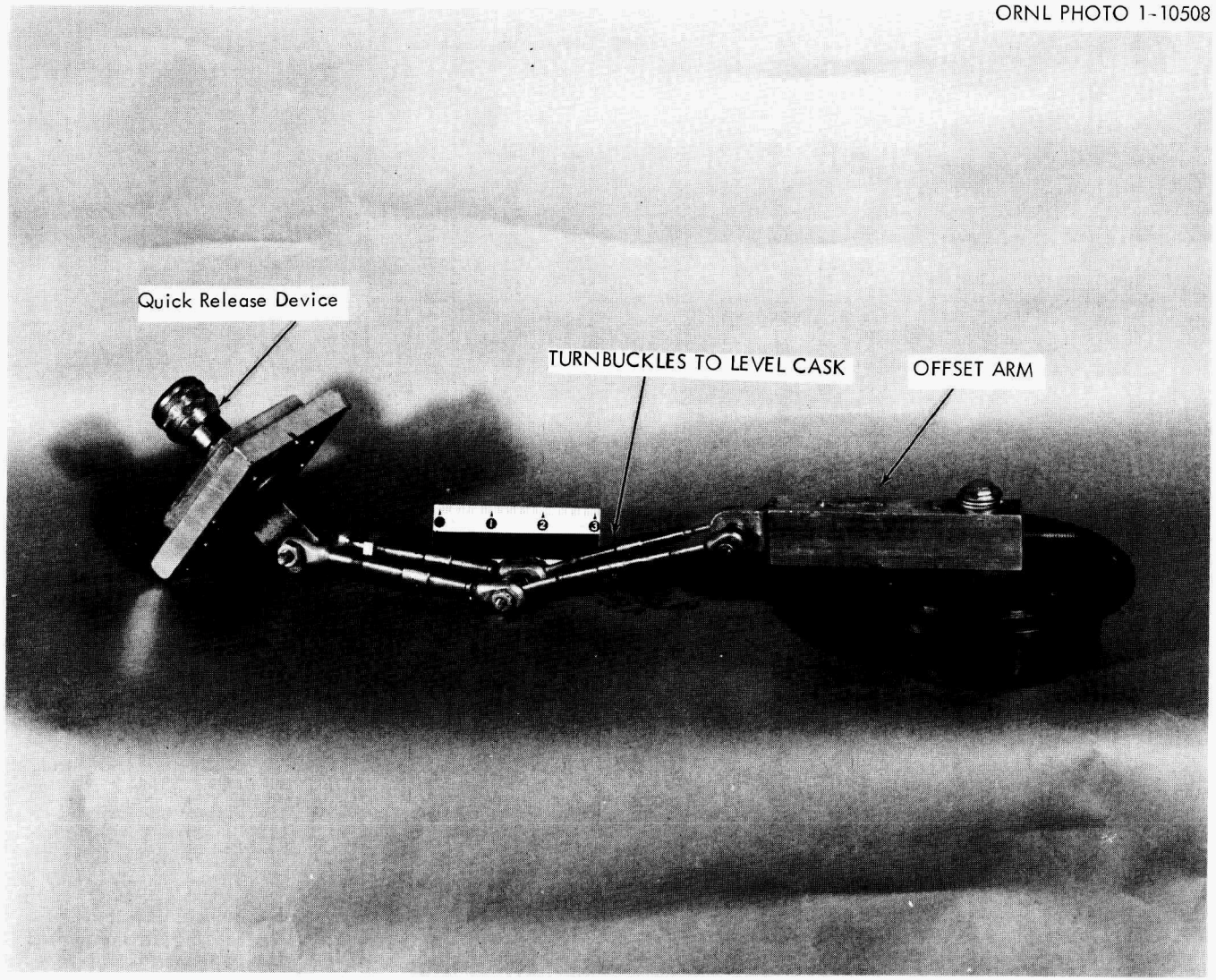

Fig. 5. Quick Release Device.

An offset arm, as shown in Fig. 5, is used for attitude control of corner drops and the turnbuckles are used to level the cask.

3.4 Data Acquisition

Data is acquired through direct measurement on the casks before and after dropping and through the use of high-speed movies using a grid as a back drop. The movies of this test were taken at 2,000 frames per second.

4. CASK TESTS – ORNL – U. T.

A test model cask was fabricated at ORNL and tested at the facility at the University of Tennessee. It was designed to model the Hallam cask designed by Atomics International and built by Allied Engineering Company, Alameda, California.

Exact test model dimensions in relation to the Hallam cask are shown in Table 1 but the approximate overall scale factor was 1 to 7.5. A cut-away illustration of the test cask is shown in Fig. 6.

Table 1. Comparison of Dimensions of ORNL Built Model to Hallam Cask Dimensions

	ORNL Model Dimensions	Hallam Cask Dimensions	Ratio
Cask overall height	30-3/8 in.	237.38 in.	1:7.81
Outer shell thickness	0.202 in.	1.50 in.	1:7.43
Inner shell thickness	0.095 in.	.75 in.	1:7.89
Lead thickness	0.936 in.	7-1/4 in.	1:7.75
Lead fill height	27-5/64 in.	214 in.	1:7.90
Overall diameter outside	4.900 in.	37.25 in.	1:7.60
Inside diameter cavity	2.435 in.	18-1/4 in.	1:7.49
Cask weight	163 lb	71,130 lb	$1:(7.60)^3$
Distance bottom of cask to first girth weld	1-55/64 in.	13.88 in.	1:7.47

ORNL DWG 67-12865

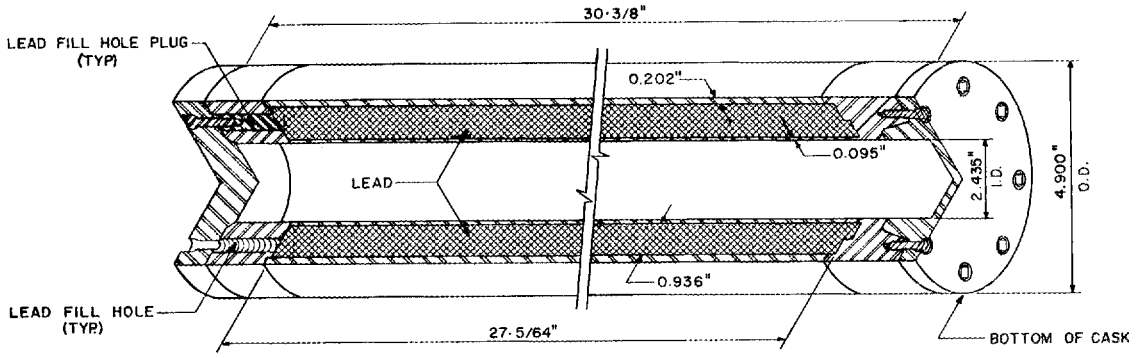

Fig. 6. ORNL Constructed 1:75 Model of the Hallam 6 Element Shipping Cask (HNPF).

The cask is shown assembled in Figs. 7 and 8. The bottom end closure is shown in Fig. 9. The top closure and the lead fill holes are shown in Fig. 10.

This cask was dropped 30 ft at the U. T. test drop facility. It was intended to drop the cask vertically so that it would hit squarely on its end. A frame from the high-speed movies at the time of impact is shown in Fig. 11 and shows that the cask actually hit at an angle of 4°32' from the vertical. Measurements of the deformation of the bottom end closure plate confirms that the angle was approximately 4°. In Fig. 11, formation of a bulge in the outer wall directly above the point of impact is clearly visible.

Both the inside and outside of the cask were smooth and no deformation occurred on the side 180 degrees away from the point of impact, while directly above the point of impact both the outside and inside steel shell walls were deformed. The deformation of the outside wall was a pronounced bulge which can be seen in Fig. 12. Deformation of the inside wall was in the form of a wrinkle which is clearly visible in the same figure.

The cask measured 30-3/8 in. long before the drop test. After the drop test the length of the cask was measured at the point of impact (presumed to be coincidental with the maximum deformation) to be 30-3/16 in. indicating a decrease of 3/16 in. At points 90 degrees on either side of the impact point, the cask length decreased by 1/8 in. Opposite the point of impact, the length of the cask shortened slightly, approximately 1/32 in.

Measurements of the outside diameter were made at three point pairs 60 degrees apart, at nine positions along the length of the cask both before and after the drop (see Table 2).

An exaggerated plot of the differences, along the three planes, determined by the point pairs as noted in Table 2, is shown in Fig. 13. It was assumed in drawing these plots that all the deformation occurred in two quadrants of the outer shell, and this is justified by close examination of the model cask after the drop.

ORNL PHOTO 88252

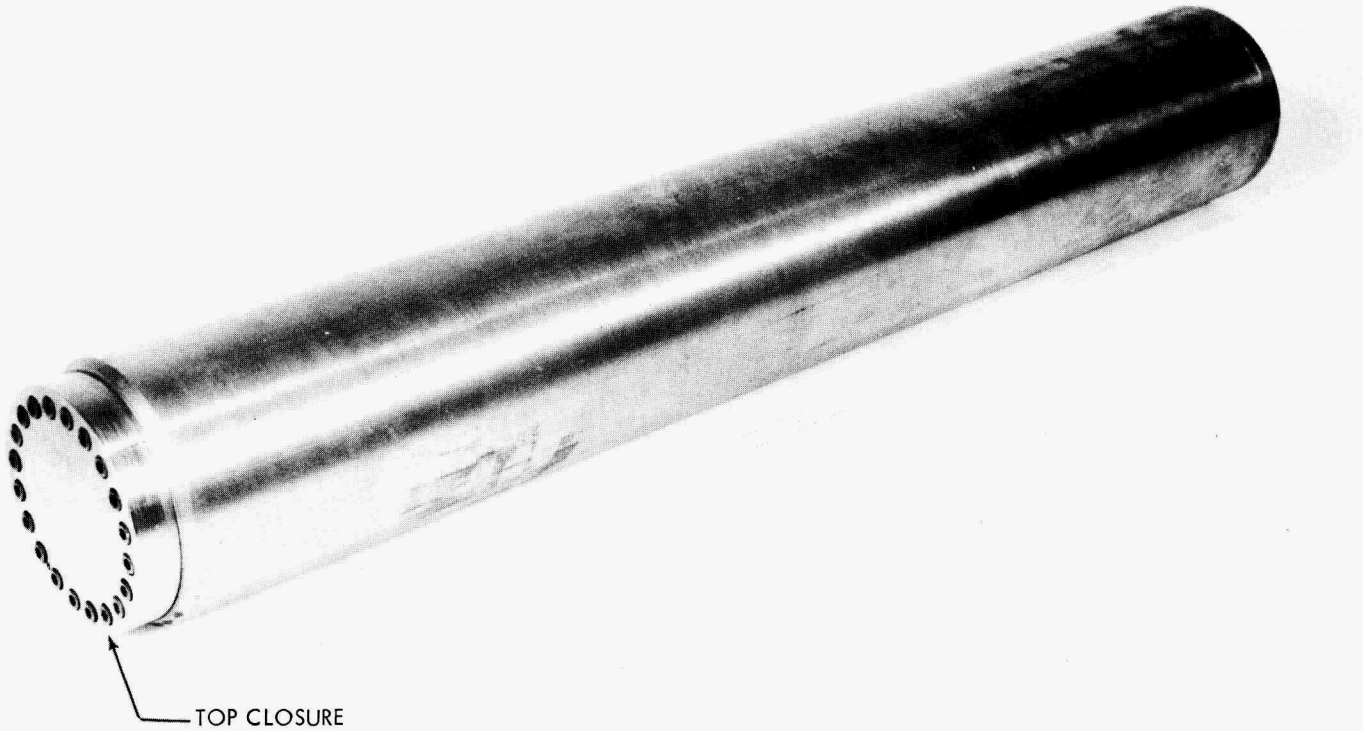

Fig. 7. ORNL-Built 1:7.5 Scale Model Test Cask of Hallam HNPF - Six-Element Shipping Cask.

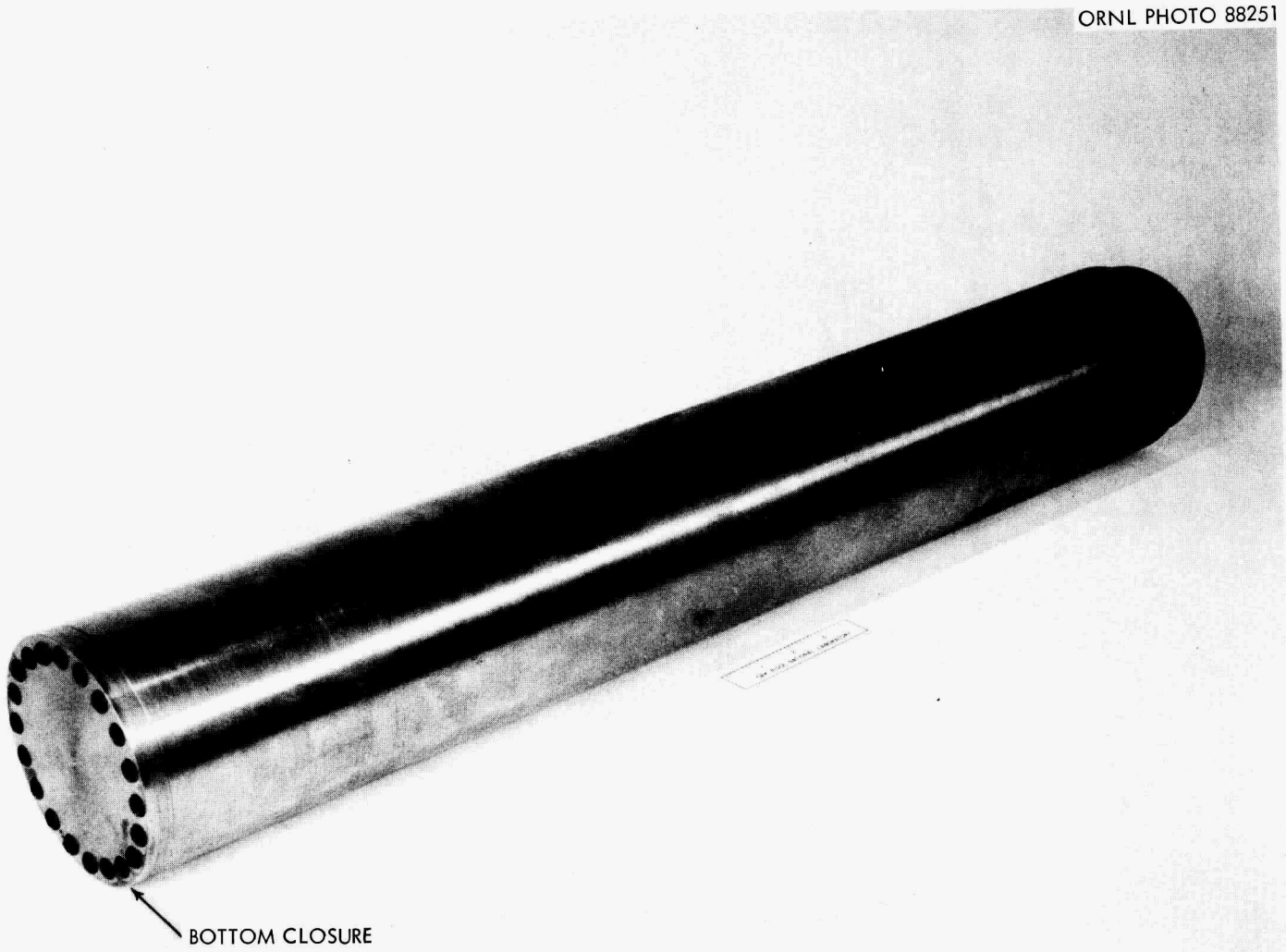

Fig. 8. ORNL-Built 1:7.5 Scale Model Test Cask of Hallam HNPF - Six-Element Shipping Cask.

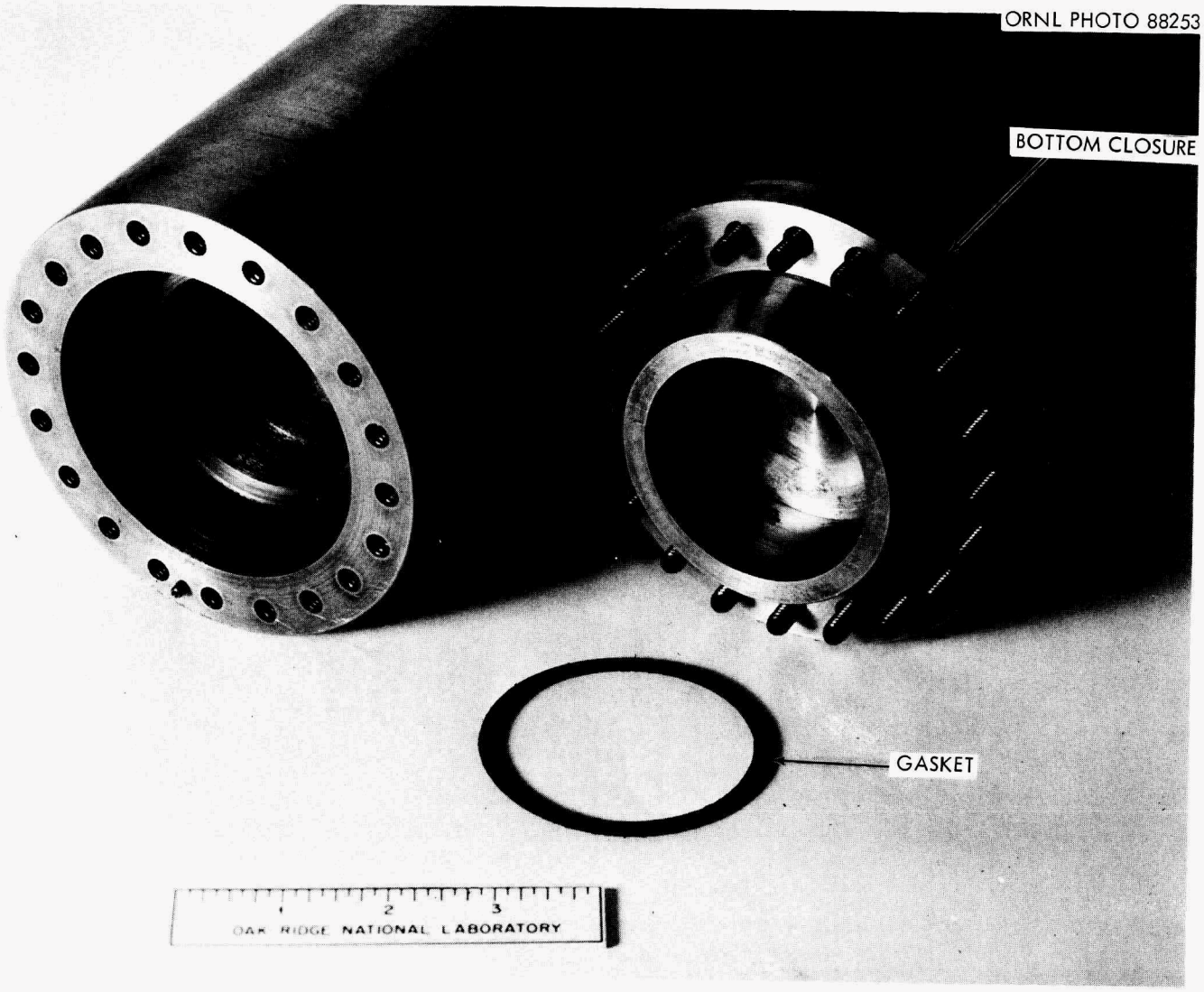

Fig. 9. ORNL-Built 1:7.5 Scale Model Test Cask of Hallam HNPF - Six-Element Shipping Cask.

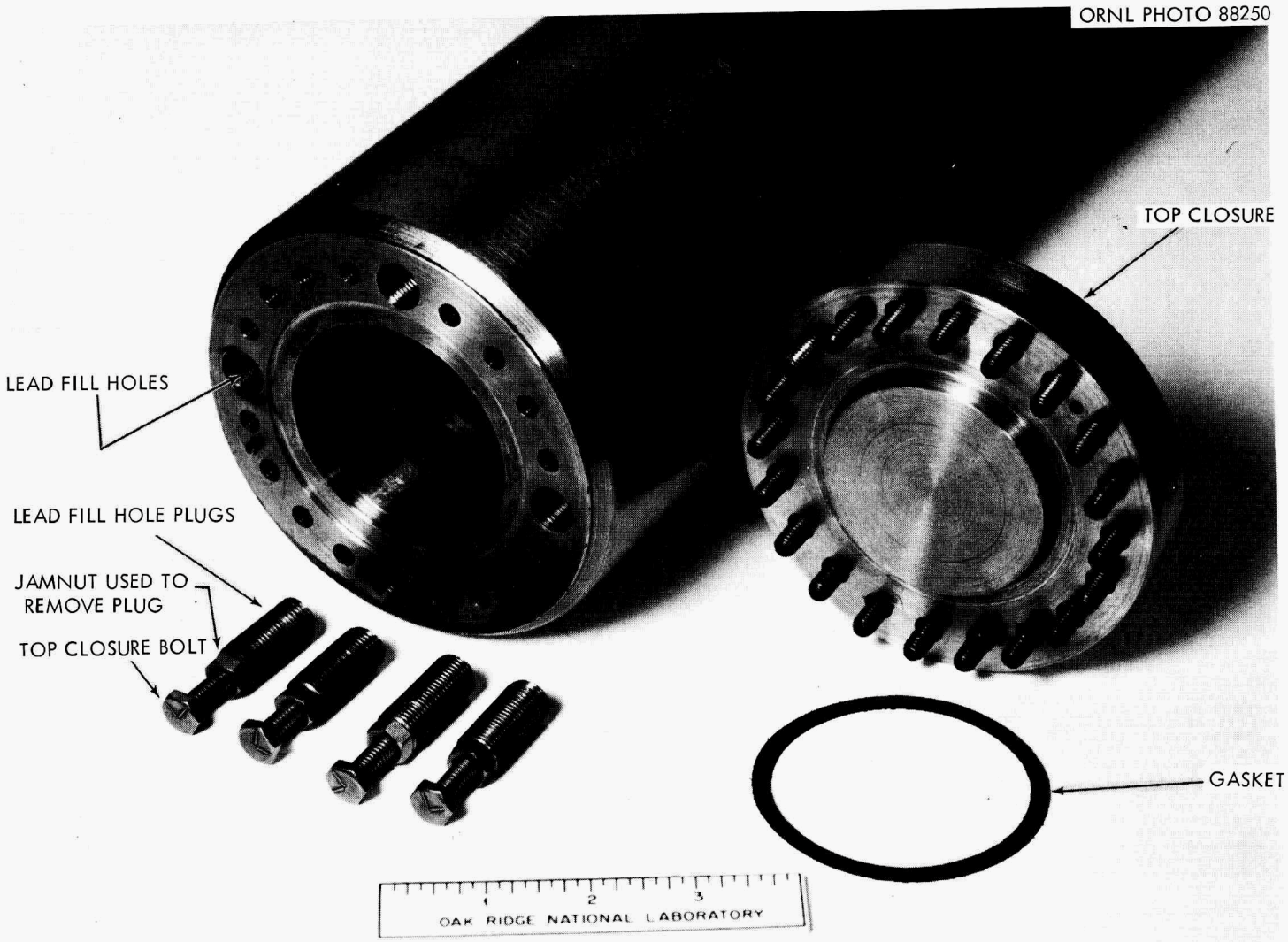

Fig. 10. ORNL-Built 1:7.5 Scale Model Test Cask of Hallam HNPF - Six-Element Shipping Cask - Top.

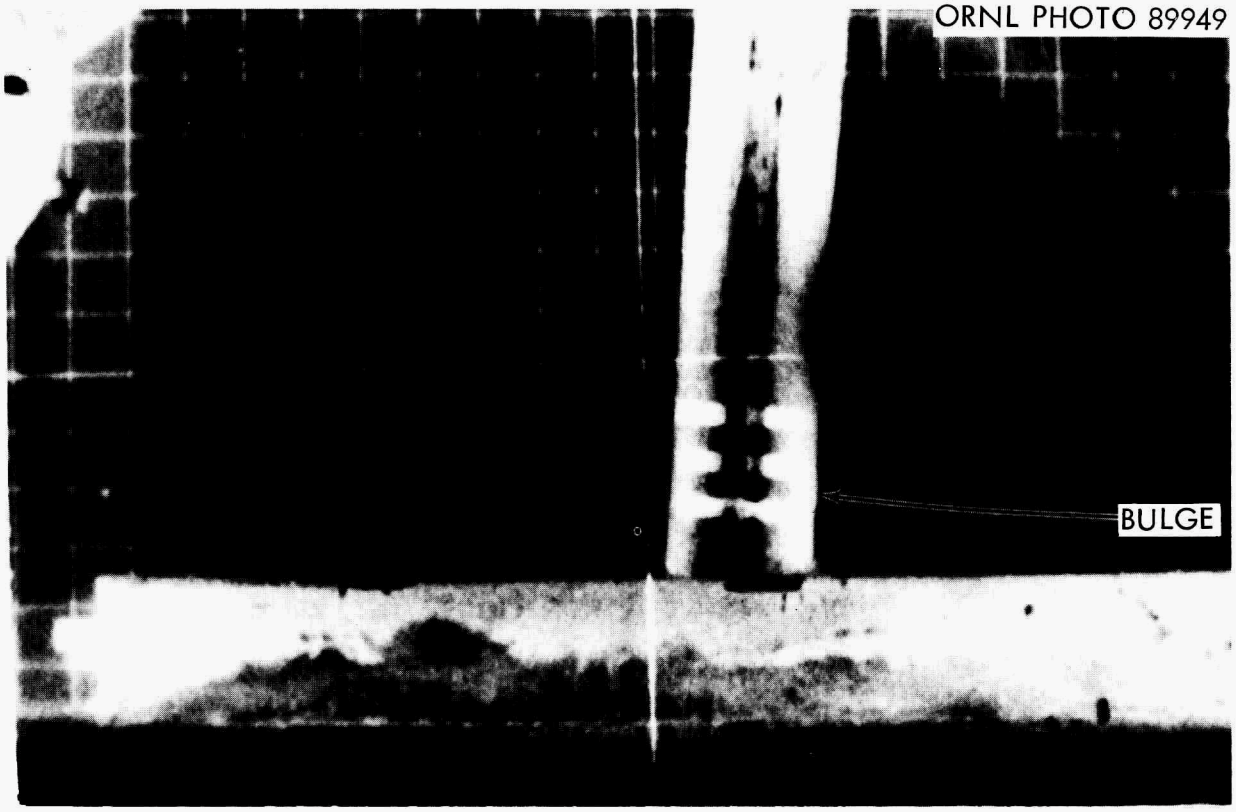

Fig. 11. ORNL - Test Cask Drop. Single frame from high-speed movies. Three frames after impact.

PHOTO 90014

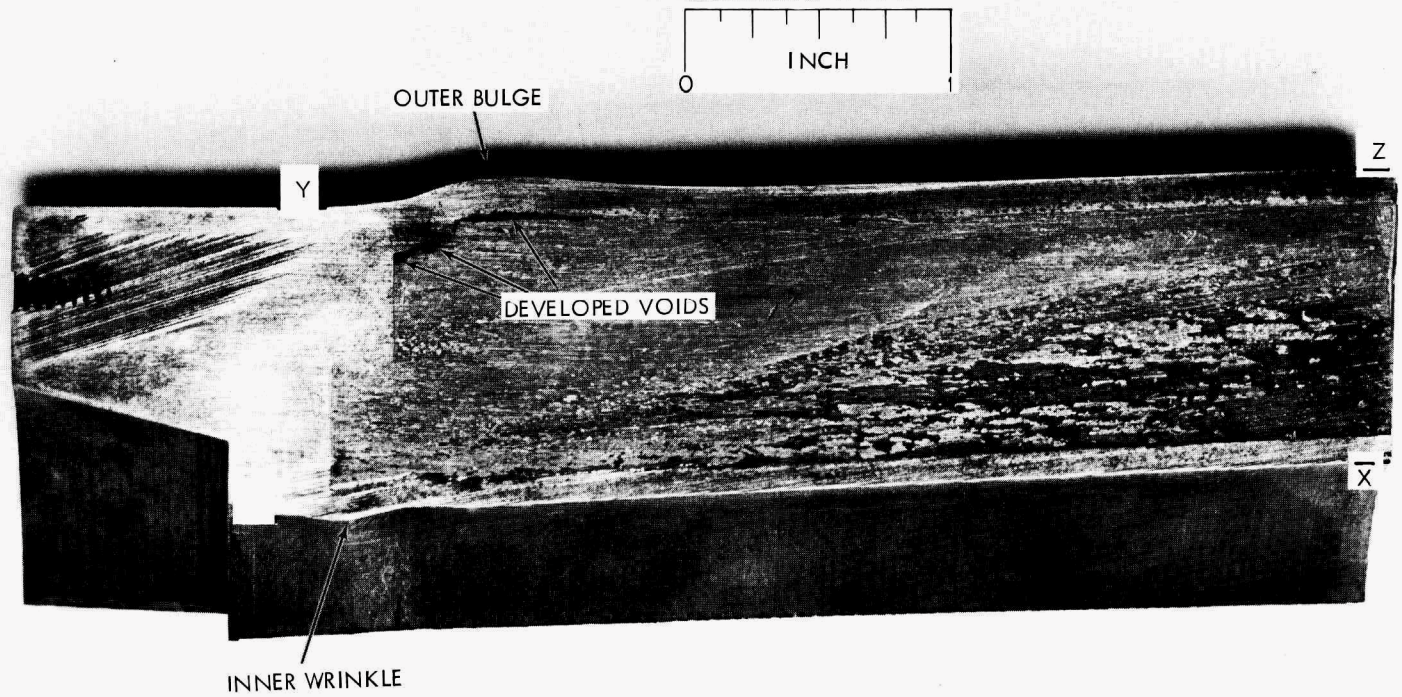

Fig. 12. Section through Maximum Deformation (G-H Figure 13).

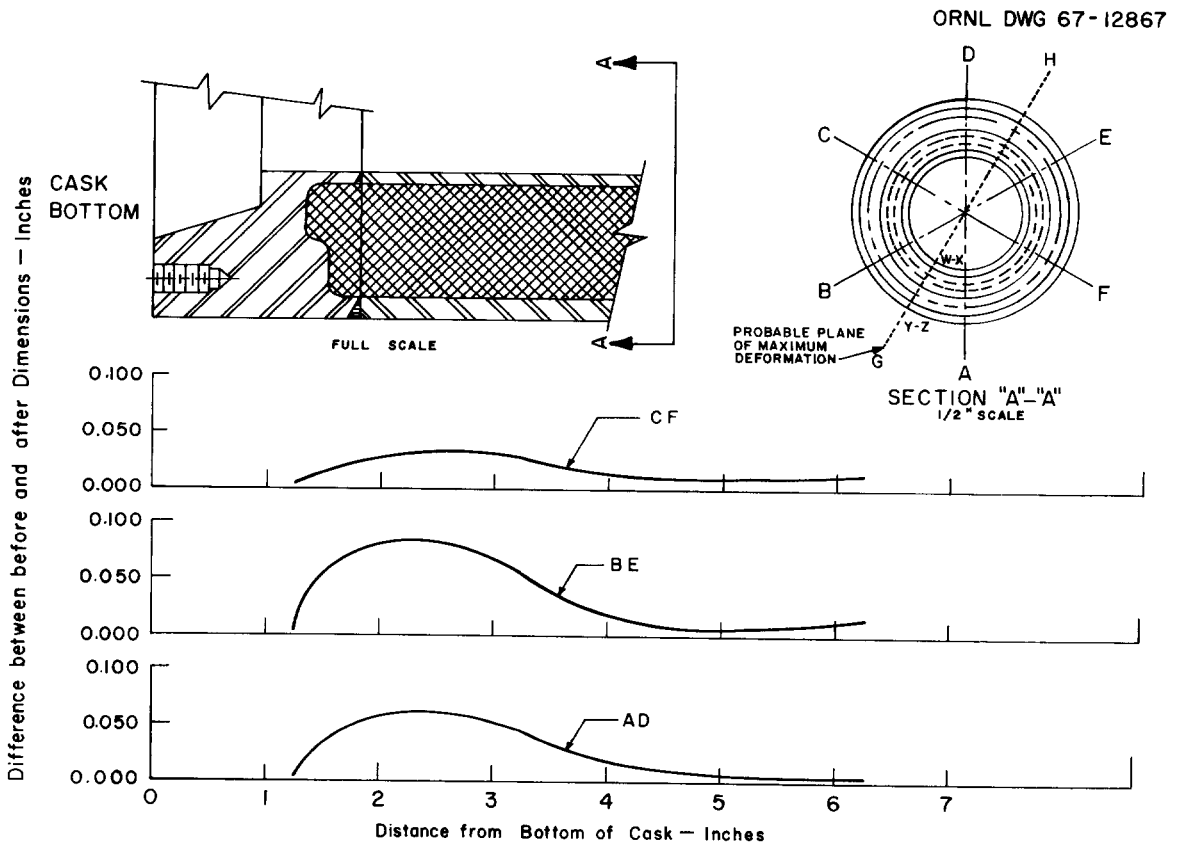

Fig. 13. Plot of Dimensions taken before and after Drop Test.

Table 2. Cask Dimensions Taken Before and After Drop Test

Distance From Bottom of Cask In.	Point Pair* AD			Point Pair* BE			Point Pair* CF		
	Before	After	Difference	Before	After	Difference	Before	After	Difference
1-1/4	4.902	4.906	+.004	4.901	4.907	+.006	4.901	4.907	+.006
2-1/4	4.901	4.962	+.061	4.901	4.987	+.086	4.901	4.940	+.039
3-1/4	4.900	4.945	+.045	4.901	4.952	+.051	4.901	4.939	+.038
4-1/4	4.899	4.915	+.016	4.900	4.911	+.011	4.900	4.912	+.012
5-1/4	4.895	4.899	+.044	4.897	4.907	+.010	4.896	4.907	+.011
6-1/4	4.891	4.893	+.002	4.893	4.908	+.015	4.892	4.907	+.015
7-1/4	4.891	4.890	-.001	4.893	4.911	+.018	4.892	4.911	+.019
8-1/4	4.891	4.893	+.002	4.893	4.915	+.022	4.892	4.914	+.022
9-1/4	4.891	4.8935	+.002	4.893	4.916	+.023	4.892	4.917	+.025

*See Fig. 13 for orientation.

Since impact apparently occurred between points A and B none of the plots shown in Fig. 13 correspond to the maximum deformation. Such measurements were made, however, when the cask was sectioned through the maximum deformation, thought to correspond to the plane labeled G-H in Fig. 13. A photograph of the section through the maximum deformation (Fig. 12) clearly shows voids between the lead and the outer shell which was formed as a result of the impact. Also shown is the wrinkle in the inner shell. Dimensions were taken of the inside and outside surfaces to determine deflections in the metal. Lack of pre-defined references necessitated choice of artificial lines for these dimensions. The reference used to measure the outer shell was determined by a straight line running between the two points marked Y and Z (Fig. 12) and on the inner shell by points W and X (Fig. 12). These two reference lines are based on four points which are believed to have moved very little. Tabulation of the data is given in Table 4 and the data is shown in an exaggerated plot beside a sketch of the cask in Fig. 14.

The distance from the top of the cask to the lead surface was measured through the lead fill holes before and after the drop test (see Fig. 10); the data are presented in Table 3.

Table 3. Measurements of Lead Position
Before and After Drop Test Measured from Top of Cask

Fill Hole Designation	Distance from Top of Fill Hole Inches		Lead Settlement Inches
	Before Drop	After Drop	
A	1.723	2.413	0.695
B	2.023	2.723	0.700
C	1.740	2.442	0.702
D	1.724	2.413	0.689

Radiographs taken before and after the drop confirm the distance of the lead settlement and the fact that the lead settled uniformly.

Table 4. Dimensions* Taken of ORNL Test Cask at Section Through Maximum Deformation

Outer Edge**		Inner Edge***	
Distance From Bottom End	Deviation (Inches)	Distance From Bottom End	Deviation (Inches)
0	.0525	15/16	-.0045
1/4	.0415	1-1/16	-.0021
1/2	.0308	1-3/16	+.0041
3/4	.0195	1-5/16	+.0245
1.000	.0096	1-7/16	+.0380
1-1/4	0.	1-9/16	+.0156
1-1/2	.0056	1-11/16	-.0045
1-3/4	.0478	1-15/16	+.0067
2.000	.0988	2-1/16	+.0072
2-1/4	.0850	2-3/16	+.0067
2-1/2	.0532	2-5/16	+.005
2-3/4	.0312	2-7/16	+.0038
3.000	.0119	2-9/16	+.0023
3-1/4	.0134	2-11/16	+.002
3-1/2	.010	2-13/16	+.001
3-3/4	.004	2-15/16	+.001
4.000	.004	3-1/16	0.
4-1/4	.002	3-3/16	0.
4-1/2	0.	3-5/16	-.001
4-3/4	0.	3-7/16	-.0015
5.000	0.	3-9/16	-.0015
5-1/4	0.	3-11/16	-.0018
5-1/2	0.	3-13/16	-.0015
		3-15/16	+.001
		4-1/16	+.001
		4-3/16	0.
		4-5/16	0.
		4-7/16	0.
		4-9/16	0.
		4-11/16	0.
		4-13/16	0.

*These dimensions are taken from two arbitrary reference lines.

**Outer edge line through Y-Z.

***Inner edge line through W-X.

ORNL DWG. 67-12876

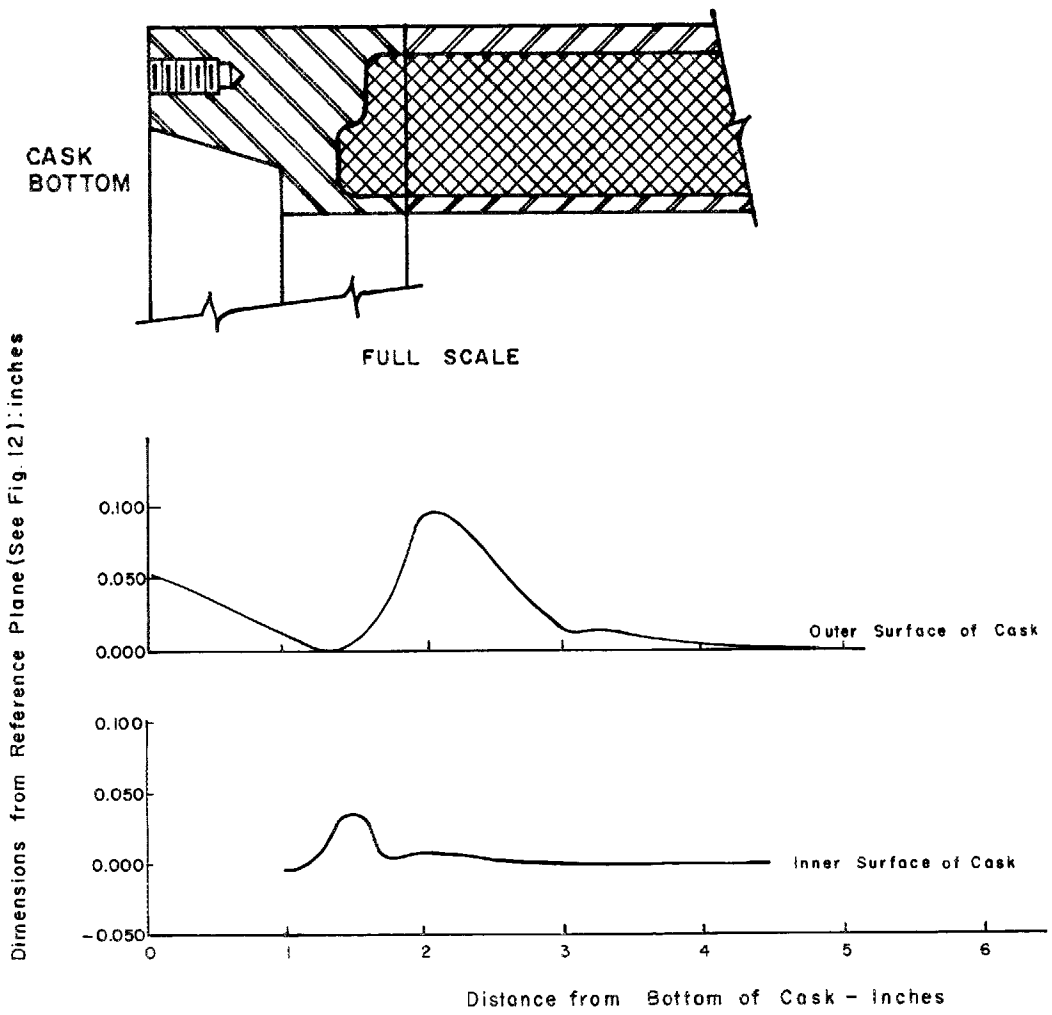

Fig. 14. Plot of Dimensions taken of Section Through Maximum Deformation

5. CASK TESTING – FRANKLIN INSTITUTE

A small model (see Fig. 15) of a radioactive material shipping cask was subjected to impact tests to investigate lead settling at Franklin Institute Research Laboratories[2]. The lead was not bonded to the mild steel shell. The cask, oriented vertically, was dropped from a height of 30 ft onto a massive steel anvil. The lead settled a distance of 0.409 in. which is equal to 2.3% of its initial height. This test data is compared to an analytical examination of the drop in Sect. 8.

6. ANALYTICAL TREATMENT OF LEAD MOVEMENT UNDER IMPACT CONDITIONS

The kinetic energy of a cask at impact must be dissipated either in the cask or its environment before it will come to rest. Since regulations stipulate the impact surface must be essentially unyielding, virtually all the energy must be absorbed by elastic and plastic deformation of material which may or may not be part of the cask proper. The material properties under dynamic conditions must therefore be known in order to analytically study the effect of impact on the cask.

Since tests to determine properties of ferrous materials at the strain rates expected during impact indicate that relatively small increases in the yield point stress levels are experienced,[3,4] it is recommended that the static yield point stress be used for steel shells, heads, flanges, etc. in the determination of plastic deformations.

The dynamic properties of lead have been investigated many times and some of the references and their findings are presented. The mechanical properties of chemical lead under static conditions at room temperature are as follows[5]:

	Cast lead
Modulus of elasticity	2×10^6 psi
Poisson's ratio	.40 to .45
Tensile strength	2300 - 2800 psi
% Ultimate elongation	~ 33%
Brinell hardness No.	4.0 - 6.0

ORNL DWG. 67-12889

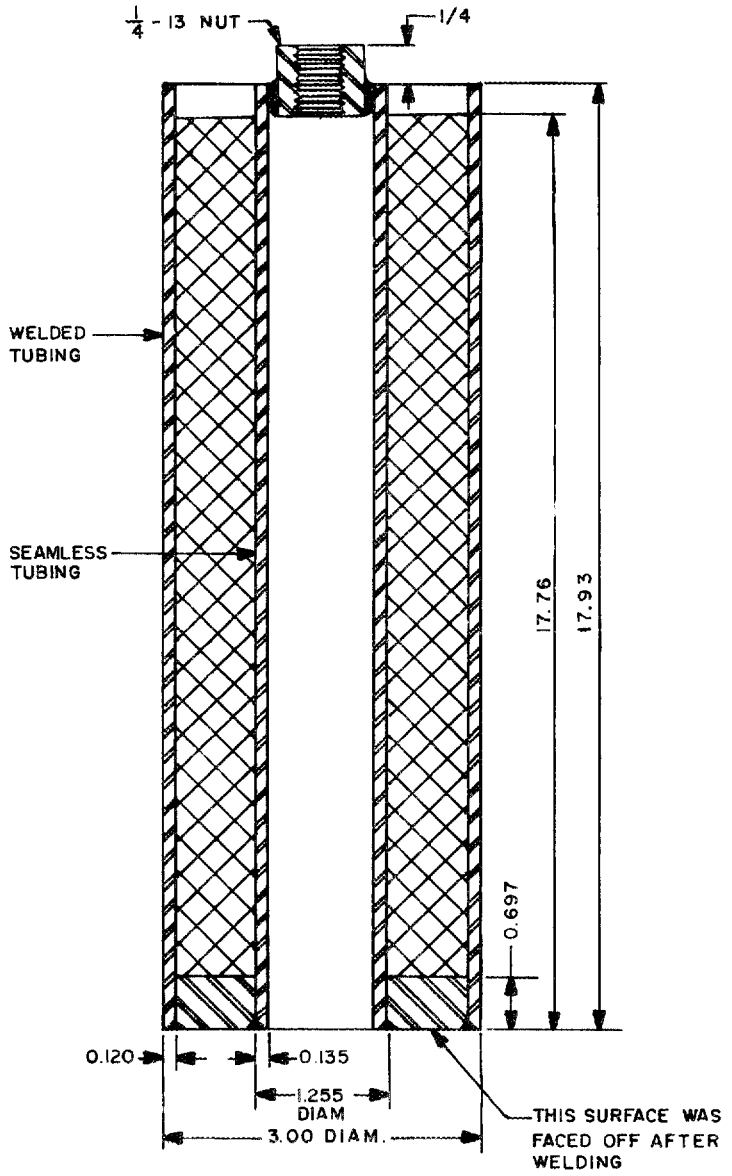

ALL DIMENSIONS IN INCHES. NOT TO SCALE.

Fig. 15. Drawing of Franklin Institute Research Laboratory Test Cask Model 22.

Based on Brinell hardness number of 4.0, the static flow pressure of lead has been calculated to be 5900 psi. The dynamic flow pressure, defined as the amount of energy required to displace a unit volume of material under dynamic conditions is reported by several investigators to be higher than this value.

The dynamic flow pressure of common plumbers lead as measured by J. H. Vincent[6] was found to be between 8700 psi and 18,850 psi; this wide range was attributed to variations in the crystal size or orientation and possibly material impurities. Another investigator, J. P. Andrews[7,8], found that the impact energy versus apparent removal of material, i.e., displaced volume, plotted as a straight line in the range of velocities investigated for a particular sample of material. Clarke, in another study[9] presents a nondimensional strain factor as a function of impact velocity; this factor may be readily converted to a dynamic flow pressure. By using his definition of radial strain, a value of 8500 psi for the dynamic flow pressure of lead may be calculated.

These data indicate that lead tends to resist deformation under dynamic conditions more than under equivalent static conditions; for example, it was assumed in ref. 7 that the energy required to displace one cubic inch of lead is approximately four times the static tensile strength. This assumption is also verified approximately in ref. 10, which gives a value of 10,300 psi for the dynamic flow pressure.

From the above data it is clear that the dynamic flow pressure of lead is a relatively uncertain quantity dependent upon test specimen configurations and methods of correlation. A reasonable and conservative value which may be used appears to be the static flow pressure of lead, or about 5900 psi.

6.1 End Drop

A limited amount of test data indicates that the steel weldments of a lead-shielded cylindrical cask constructed with full penetration welds will withstand a 30-ft impact on end without rupture or excessive distortion of the shells. If the end drop is perpendicular to the drop pad,

then the lead, if unbonded, will receive little support from either the inner or outer shell; the lead will then settle its maximum amount, possibly creating a void in the annular shielding cavity opposite the end of impact.

Assuming lead to be an incompressible medium and considering a toroidal element, in which the diameter of the inner hole does not change under an axial force (Fig. 16), the radial strain is found to be related to the axial strain as noted in Eq. 6.1.

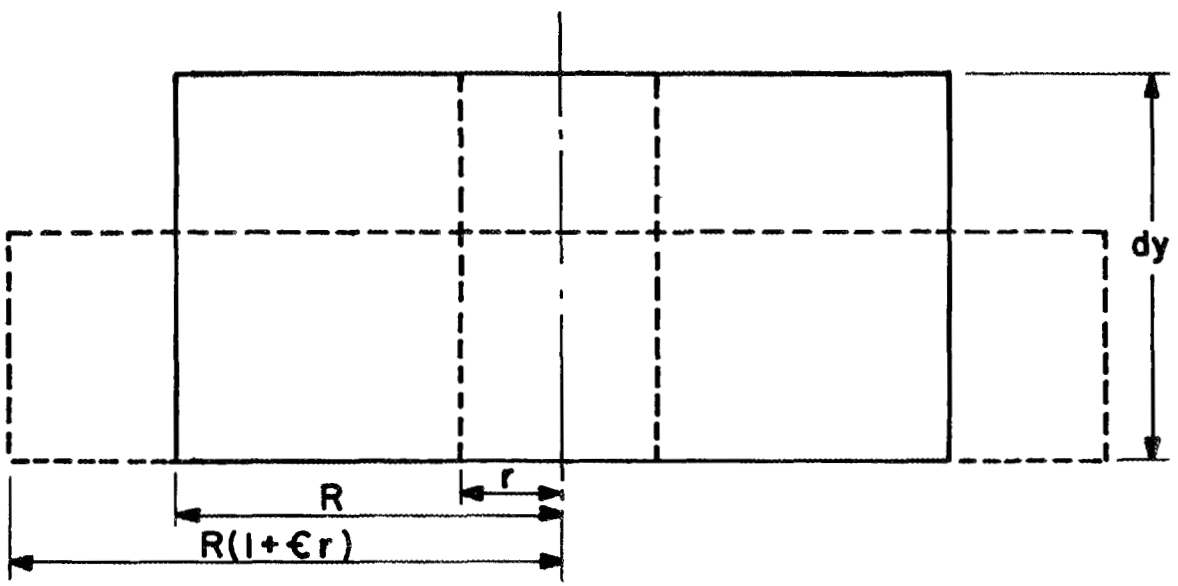

Fig. 16. Schematic Drawing of a Toroidal Element

That is,

$$\pi(R^2 - r^2)\ dy = \pi[R^2\ (1 + \varepsilon_r)^2 - r^2]\ (1 - \varepsilon_y)\ dy \qquad (6.1)$$

where

ε_r = increase in radius due to settlement of lead divided by the original radius,

ε_y = decrease in length of lead due to settlement divided by the original length,

r = inner radius of original lead,

R = outer radius of original lead,

dy = incremental length of lead.

By simplifying Eq. 6.1 and neglecting all higher order infinitesimals, it can be shown that:

$$\varepsilon_y = 2\,\varepsilon_r \left(\frac{R^2}{R^2 - r^2}\right) \tag{6.2}$$

The strain energy in the lead may be calculated by:

$$E_{pb} = \int_0^{\ell} \sigma_{pb}\, \pi[R^2\ (1 + \varepsilon_r)^2 - r^2]\ \varepsilon_y dy \tag{6.3}$$

where

R = outer radius of lead,

r = inner radius of lead,

σ_{pb} = dynamic flow stress in lead,

E_{pb} = the strain energy absorbed in the lead,

ℓ = overall length of lead.

Rearranging Eq. 6.3 after substituting from Eq. 6.2 for ε_y

$$E_{pb} = 2\pi\sigma_{pb}R^2 \int_0^{\ell} \varepsilon_r dy \tag{6.4}$$

The strain energy absorbed in the outer shell of the cask, E_s, may be calculated as follows:

$$E_s = \int_0^{\ell} \sigma_s t_s\ (2\pi R)\ \varepsilon_c dy \tag{6.5}$$

where

σ_s = tensile strength of outer shell material,

ε_c = the circumferential strain in the shell,

t_s = thickness of outer shell.

This leads to:

$$E_s = 2\pi R t_s \sigma_s \int_0^{\ell} \varepsilon_r dy \tag{6.6}$$

since

$\varepsilon_r = \varepsilon_c$ for a cylindrical shell.

The two energies given by Eqs. 6.4 and 6.6 must equal the kinetic energy of the cask at impact. If the maximum strain is actually desired one must now choose a form for the outer shell deflection curve in order to evaluate the integral. If the change in volume of the annular cavity is desired, it may be determined without evaluating the integral by considering the following:

$$\Delta V = \int_0^{\ell} \pi[R^2 (1 + \varepsilon_r)^2 - R^2] \, dy \tag{6.7}$$

where

ΔV = the void volume created by the displacement of lead,

ℓ = original length of the volume of lead.

This equation simplifies to

$$\Delta V = 2\pi R^2 \int_0^{\ell} \varepsilon_r \, dy \tag{6.8}$$

when higher order infinitesimals are neglected.

Since all kinetic energy must be absorbed in the cask as noted above, Eqs. 6.4 and 6.6 may be combined as noted below:

$$WH = (2\pi R t_s \sigma_s + 2\pi R^2 \sigma_{pb}) \int_0^{\ell} \varepsilon_r \, dy \tag{6.9}$$

where

W = weight of the cask,

H = height of drop.

Rearranging Eq. 6.9, we have

$$\int_0^{\ell} \varepsilon_r \, dy = \frac{WH}{2\pi(Rt_s\sigma_s + R^2\sigma_{pb})} \tag{6.10}$$

Rearranging Eq. 6.8

$$\int_0^{\ell} \varepsilon_r \, dy = \frac{\Delta V}{2\pi R^2} \tag{6.11}$$

Combining Eqs. 6.10 and 6.11 gives:

$$\Delta V = \frac{R^2 WH}{Rt_s\sigma_s + R^2\sigma_{pb}} \tag{6.12}$$

Since the change in the height of the lead column, Δh caused by the impact is:

$$\Delta h = \frac{\Delta V}{\pi(R^2 - r^2)} \tag{6.13}$$

then

$$\Delta h = \frac{R^2}{\pi(R^2 - r^2)} \left(\frac{WH}{Rt_s\sigma_s + R^2\sigma_{pb}}\right) \tag{6.14}$$

It should be reemphasized that Eq. 6.14 cannot be used if the lead is bonded to the steel shells since support is provided that is not taken into account.

7. APPLICATION OF ANALYSIS TO ORNL-BUILT 1:7.5 SCALE MODEL OF HALLAM CASK

Data was obtained during the drop test of the 1:7.5 scale model of the Hallam cask. While the drop was not quite flat onto its end, it will be treated here as though it was. Pertinent data of the cask used to analyze the lead movement problem is given below:

$W = 163$ lb,

$H = 30$ ft or 360 in.,

$R = 2.248$ in.

$r = 1.3125$ in.,

$t_s = 0.20$ in.,

$\sigma_s = 45{,}000$ psi (seamless cold drawn tubing),

$\sigma_{pb} = 5500$ psi (This dynamic flow pressure was assumed. It is close to the static flow pressure discussed on page 26).

From Eq. 6.14

$$\Delta H = \frac{(2.25)^2\ (163)\ (360)}{\pi[(2.25)^2 - (1.31)^2]\ [(2.25)\ (0.20)\ (45000) + (2.25)^2\ (5500)]}$$

$= .59$ in. settlement

Experimental data of this drop indicated the lead actually was displaced 0.7 in. which is in reasonable agreement with that predicted above. The lead displacement of 0.7 in. is equivalent to a reduction in the length of the contained lead column of 2.6%.

8. APPLICATION OF ANALYSIS TO THE FRANKLIN INSTITUTE 1:12.5 SCALE MODEL OF HALLAM CASK

Data was obtained during the drop test of the 1:12.5 scale model of the Hallam cask.

Pertinent data of the cask used to analyze the lead movement problem are given below:

	Model 22
$W =$	41.52 lb,
$H =$	30.00 ft or 360 in.,
$R =$	1.380 in.,
$r =$	0.628 in.,
$t_s =$	.120 in.,
$\sigma_s =$	45,000 psi,
$\sigma_{pb} =$	5500 psi

From Eq. 6.14

$$\Delta H_{22} = \frac{(1.380)^2\ (41.52)\ (360)}{\pi[(1.380)^2 - (0.628)^2]\ [(1.380)(0.120)(45000) + (1.380)^2\ (5500)]}$$

$= .335$ in. settlement

The test cask Model 22 actually had a lead displacement of 0.409 in. which is in reasonable agreement with the calculated 0.335 in. The lead displacement of 0.409 in. is equivalent to a reduction in the length of the contained lead column of 2.3%.

9. ACKNOWLEDGEMENT

We would like to express our appreciation to D. C. Watkin for the model cask design and to Prof. R. L. Shobe, C. T. Welch, and F. E. Shadid as members of the University of Tennessee staff for their help in the drop test of the model cask.

REFERENCES

1. AEC Manual, Chapter 0529, Safety Standards for the Packaging of Radioactive and Fissile Materials, Aug. 22, 1966.

2. H. G. Clarke, Jr. and S. P. Carfagno, Structural Integrity of Shipping Containers for Radioactive Material, Part IX Test of Settling of Lead Shielding due to End Impact, FIRL Interim Report I-A2412-9 and USAEC Report NYO-2539-8.

3. J. Marin, Engineering Materials, p. 231, Prentice-Hall, Inc., N. Y., 1952.

4. D. W. Goodpasture and L. B. Shappert, Energy Absorption Capability of Steel Determined from Cask Impact Tests, p. 48, ORNL-TM-680, Jan. 1964.

5. Lead in Modern Industry, Lead Industries Association, New York, 1952.

6. J. H. Vincent, Proc. Camb Phil Soc X, p. 332 (1898 - 1900).

7. J. P. Andrews, Phil Mag S.7 Vol 8 No. 53 Suppl Dec. 1929.

8. J. P. Andrews, Phil Mag S.7 Vol 9 No. 58 April 1930.

9. H. G. Clarke and W. E. Onderko, "Model Impact Tests Pertaining to Shipping Containers," Summary Report on AEC Symposium on Packaging and Regulatory Standards for Shipping Radioactive Materials, Germantown, Md., Dec. 3-5, 1962, TID-7651, p. 238.

10. L. B. Shappert, A Guide to the Design of Shipping Casks for the Transportation of Radioactive Material, ORNL-TM-681, April 1965.

Internal Distribution

1. T. A. Arehart
2. M. Bender
3. C. E. Bettis
4. R. E. Blanco
5. R. E. Brooksbank
6. K. B. Brown
7. F. R. Bruce
8. J. R. Buchanan
9. C. D. Cagle
10. F. L. Culler, Jr.
11. R. L. Donahue
12. H. G. Duggan
13. J. H. Evans
14. D. E. Ferguson
15. W. R. Gall
16. J. H. Gillette
17. H. E. Goeller
18. K. W. Haff
19. R. L. Jolley
20. O. A. Kelly
21. E. M. King
22. B. B. Klima
23. A. J. Mallett (K-25)
24. J. R. McGuffey
25. J. D. McLendon (Y-12)
26. H. A. Nelms
27. J. P. Nichols
28. R. Salmon
29. W. F. Schaffer
30. R. D. Seagren
31-40. L. B. Shappert
41-45. W. C. Stoddart
46. D. A. Sundberg
47. W. E. Unger
48. D. C. Watkin
49. M. E. Whatley
50. R. G. Wymer
51-52. Central Research Library
53. Document Reference Section
54. GE&C Division Library
55-62. Laboratory Records Department
63. Laboratory Records, ORNL R.C.
64. ORNL Patent Office

External Distribution

65. R. F. Barker, AEC, Washington, D. C.
66. D. E. Beaderstadt, Chicago Operations Office
67. C. Beck, AEC, Washington, D. C.
68. W. G. Belter, AEC, Washington, D. C.
69. H. G. Clarke, Franklin Institute
70. G. C. Gower, Chicago Operations Office
71. J. C. Glynn, AEC, Washington, D. C.
72. Robert Jetter, Atomics International
73. W. A. Johnson, AEC, Oak Ridge
74. John Langhaar, DuPont, Wilmington
75. J. A. Lenhard, AEC, Oak Ridge
76. J. A. Lieberman, AEC, Washington, D. C.
77. B. G. Lindberg, AEC, Washington, D. C.
78. E. Lusk, Battelle Memorial Institute
79. W. A. Nelson, AEC, Washington, D. C.
80. D. E. Patterson, AEC, Washington, D. C.
81. R. W. Peterson, National Lead, Wilmington

82. W. A. Pryor, AEC, Oak Ridge
83. T. Ricci, Atomics International
84. E. M. Shank, Eurochemic
85. L. R. Shobe, University of Tennessee
86. J. A. Sisler, AEC, Washington, D. C.
87. C. H. Weaver, University of Tennessee
88-102. Division of Technical Information Extension
103. Laboratory and University Division, ORO